AR-009-875

DSTO-TR-0409

Effect of Bonded Insert Shape and Adhesive Thickness on Critical Stresses in a Loaded Plate

R.L. Evans and M. Heller

APPROVED FOR PUBLIC RELEASE

DEPARTMENT OF DEFENCE

DEFENCE SCIENCE AND TECHNOLOGY ORGANISATION

Mar 26

Effect of Bonded Insert Shape and Adhesive Thickness on Critical Stresses in a Loaded Plate

R.L. Evans and M. Heller

Airframes and Engines Division
Aeronautical and Maritime Research Laboratory

DSTO-TR-0409

ABSTRACT

This report presents the results of finite element analyses conducted to calculate the magnitude of adhesive stresses for a large plate with a bonded insert, and study the interaction of key parameters including (i) insert shape, and (ii) adhesive modulus and thickness, with maximum plate stresses. Results are presented for circular, oval and elliptical insert cases. It is shown that changing the key variables can improve the efficiency of such repairs, however due to typically high adhesive stresses, careful consideration must be given to the level of applied loading and the design of the insert chosen. In general, for a particular shape of reinforcement, there is a trade-off between plate and adhesive stress magnitudes. This relationship is such that minimising adhesive stresses (through increasing adhesive thickness or reducing adhesive modulus) reduces the beneficial effect on plate stresses of the bonded reinforcement. It is shown that for circular inserts this relationship is essentially linear.

DEPARTMENT OF DEFENCE

DEFENCE SCIENCE AND TECHNOLOGY ORGANISATION

Published by

DSTO Aeronautical and Maritime Research Laboratory
PO Box 4331
Melbourne Victoria 3001

Telephone: (03) 9626 8111
Fax: (03) 9626 8999

AR No. AR-009-875
August 1996

APPROVED FOR PUBLIC RELEASE

Effect of Bonded Insert Shape and Adhesive Thickness on Critical Stresses in a Loaded Plate

Executive Summary

At AMRL particular attention has been given to the analysis and development of methods suitable for the life extension of aircraft components, in particular, airframes. The development of bonded composite repair technology suitable for the life extension of aircraft structures has been a specific focus. Many such repairs have been applied to aircraft in service with the Royal Australian Air Force.

Some investigations on another form of bonded reinforcement have also been undertaken, where a metallic insert is bonded into a hole, in the context of life extension of plates containing uncracked or cracked holes. One perceived scenario is that for the case of a cracked hole; the crack could be removed by hole reaming, and then an insert bonded into the resultant oversized hole. Early theoretical (finite element) and experimental investigations have indicated that (assuming the adhesive remains intact) stress concentrations and stress intensity factors can be significantly reduced, and also significant improvements in fatigue life have been demonstrated.

These promising results prompted further work on this topic by DRA and AMRL under the auspices of an AAMOUR agreement. Here testing of aluminium specimens with a bonded steel insert under both constant amplitude and FALSTAFF sequences was undertaken. However in these tests minimal or no life improvement was shown. In view of these unexpected results it was decided that AMRL work (reported herein), be directed towards quantifying the distribution and magnitude of adhesive stresses, and study the interaction of key parameters including (i) insert shape, and (ii) adhesive modulus and thickness, with maximum plate stresses.

It has been shown herein that in general, adhesive stresses are high at particular locations around the insert/plate interface. Hence to effectively use bonded inserts, careful consideration must be given to the level of applied loading and the particular design of insert. Analyses and results have been presented for circular, oval and elliptical insert cases. It has been shown that changing the key variables can improve the efficiency of such repairs. In general, for a particular shape of reinforcement, there is a trade off between plate and adhesive stresses. This is such that minimising adhesive stresses (through increasing adhesive thickness or reducing its modulus) reduces the beneficial effect on plate stresses of the bonded reinforcement. For circular insert cases this relationship is essentially linear.

Authors

R.L. Evans
Airframes and Engines Division

Rebecca Evans completed a Bachelor of Engineering in Aeronautical Engineering at the Royal Melbourne Institute of Technology in 1987. In 1988 she commenced work in Systems Division at DSTO Salisbury, where she worked on the design, analysis and testing of towed targets. Since 1992 she has been working in the Airframes and Engines Division where she has undertaken experimental and finite element analyses of metallic aircraft components, evaluating various fatigue life enhancement techniques.

M. Heller
Airframes and Engines Division

Manfred Heller completed a B. Eng. (Hons.) in Aeronautical Engineering at the University of New South Wales in 1981. He was awarded a Department of Defence Postgraduate Cadetship in 1986, completing a PhD at Melbourne University in 1989. He commenced work in Structures Division at the Aeronautical Research Laboratory in 1982. He has an extensive publication record focussing on the areas of stress analysis, fracture mechanics, fatigue life extension methodologies and experimental validation. Since 1992 he has led tasks which develop and evaluate techniques for extending the fatigue life of ADF aircraft components and provide specialised structural mechanics support to the ADF. He is currently a Senior Research Scientist in Airframes and Engines Division.

Contents

List of Abbreviations

AAMOUR	Australia -UK Memorandum of Understanding on Defence Research
AMRL	Aeronautical and Maritime Research Laboratory
DRA	Defence Research Agency (UK)
FALSTAFF	Fighter Aircraft Loading STAndard for Fatigue evaluation
PAFEC	Program for Automated Finite Element Computation

1. Introduction

At AMRL particular attention has been given to the analysis and development of methods suitable for the life extension of aircraft components, in particular, airframes. The development of bonded composite repair technology suitable for the life extension of aircraft structures has been a specific focus. Many such repairs have been applied to aircraft in service with the Royal Australian Air Force.

Some investigations on another form of bonded reinforcement have also been undertaken, where a circular metallic insert is bonded into a hole, in the context of the life extension of plates containing uncracked or cracked holes. One perceived scenario is that for the case of a cracked hole, the crack could be removed by hole reaming and then an insert bonded into the resultant oversized hole.

Finite element analyses were undertaken by Jones and Callinan [1] to investigate the repair of a cracked lug using an adhesively bonded insert. It was shown that stress intensity factors were reduced by using the bonded insert. In experimental work reported by Mann et al [2], the fatigue performance of initially uncracked specimens each containing a bonded rivet was compared to that of specimens with an open hole and holes that were cold expanded (with and without a pressed-in rivet), for a Mirage loading spectrum. Significant improvements in fatigue life were demonstrated.

In subsequent work the results of two-dimensional elastic finite element analyses of aluminium alloy plate specimens containing bonded inserts are given by Heller et al [3], who showed that if the adhesive remains intact, the stress concentration factor at a hole and the stress intensity factor at a cracked hole are significantly reduced if the hole contains a bonded rivet or bonded steel insert. For the case of aluminium alloy plates containing a hole with a bonded insert in the presence of a three dimensional flaw, the results of elastic finite element analyses were given by Heller et al [4]. It was shown (assuming the adhesive remains intact) that plate stress intensity factor is significantly reduced by using bonded steel inserts alone, or in conjunction with a bonded patch. Favourable fatigue test results under constant amplitude loading conditions for this problem are also reported by Heller et al [5].

More recently, work has been undertaken at DRA and AMRL on this topic under an AAMOUR agreement, Topic 68. In this experimental investigation, testing of specimens of similar geometry to those in [4,5] with bonded steel inserts under both constant amplitude and FALSTAFF sequences, was undertaken. Minimal or no life improvement was shown [6,7]. In view of these unexpected results it was decided that further AMRL work be directed towards quantifying the distribution and magnitude of adhesive stresses, and to study the interaction of key parameters including (i) insert shape, and (ii) adhesive modulus and thickness, with maximum plate stresses.

A description of the finite element analysis approach taken is given in Section 2. This is followed in Sections 3, 4 and 5 with analyses and results for the circular, oval and elliptical insert cases respectively. The results are then discussed in Section 6.

2. Finite element analysis approach

2.1 Geometry

The plate without reinforcement is shown in Figure 1. It is loaded by a remote stress σ_o, is of width w, and height $2h$. The centrally located hole is of radius r_h. It is assumed for the repair that an insert is bonded into the hole, as shown schematically for the case of a circular insert in Figure 2. In this work three shapes of the insert are considered, they are (i) circular (ii) oval and (iii) elliptical.

2.2 Finite element modelling

All analyses were undertaken using the PAFEC finite element package, level 7, taking linear elastic two-dimensional plane stress conditions. The computer used was a HP9000 - 755. In all finite element cases considered it was only necessary to model one-quarter of the plate due to symmetry. The following geometric, material and loading conditions were consistently used for all relevant analyses unless otherwise stated.

(i) Insert:

Young's modulus	$E_i = 200$ GPa,
Poisson's ratio	$\nu_i = 0.3$
insert inner radius	$r_{ii} = 2.9$ mm

(ii) Plate:

Young's modulus	$E_p = 70$ GPa
Poisson's ratio	$\nu_p = 0.33$
width	$w = 65$ mm
height	$2h = 65$ mm (circular hole cases)
height	$2h = 72.8$ mm (oval hole cases with $l = 3.9$ mm)
height	$2h = 88.8$ mm (oval hole cases with $l = 11.9$ mm)
height	$2h = 80$ mm (elliptical hole cases)
initial hole radius	$r_h = 4$ mm
remote stress	$\sigma_o = 115$ MPa

(iii) Adhesive:

Type A (Typical of an acrylic adhesive)
Young's modulus $E_a = 945$ MPa
Poisson's ratio $\nu_a = 0.35$

Type B (Typical of an epoxy adhesive)
Young's modulus $E_a = 2758$ MPa
Poisson's ratio $\nu_a = 0.35$

At this stage it is convenient to define the normalised maximum plate stress (NMPS) for the reinforced geometry for a particular insert shape as NMPS = K^b/K^u. Here K^b is the maximum stress concentration factor in the plate for the reinforced configuration and K^u is the maximum stress concentration factor in the plate for the unreinforced configuration. To compare different hole shape cases it must be remembered that K^u is different for each, and hence NMPS is relative only to a given hole shape.

3. Plate with bonded circular insert

3.1 Finite element modelling details

A schematic for this reinforcement case is shown in Figure 2. For all cases the plate hole radius is kept constant at $r_h = 4$ mm, and the insert inner radius is constant at $r_{ii} = 2.9$ mm, giving a nominal insert wall thickness of 1 mm. However, to accommodate cases of varying adhesive thickness around the plate hole boundary, the location of the insert/adhesive interface is allowed to vary and is defined in the cartesian co-ordinates (X, Y) as follows:

$$\left(\frac{X}{4 - t_a^{(\theta=0)}}\right)^2 + \left(\frac{Y}{4 - t_a^{(\theta=90)}}\right)^2 = 1 \tag{1}$$

The finite element mesh consisted of approximately 345, eight-noded rectangular iso-parametric elements. A typical mesh is shown in Figure 3. The adhesive was modelled using one layer of elements and both adhesive types, namely A and B, were considered.

3.2 Benchmark cases for bounding and validation

A number of preliminary analyses were undertaken using this mesh to confirm the accuracy of the model. For the open hole (unreinforced) case, the stress concentration factor was obtained as $K^u = 3.14$, as compared to $K^u = 3.05$ from Peterson [8]. A lower bound for the repaired plate stress concentration factor, K^b, can be obtained by assuming the insert is

rigidly connected to the plate; in this case the FE analysis gives $K^b = 0.91$ (for a finite width plate), while from Koplic and Klassen [9], $K^b = 0.8$ (for an infinite plate).

3.3 Analysis and results for cases with constant adhesive thickness

The adhesive stresses in polar co-ordinates (r,θ) are given in Figures 4 and 5 for the two adhesives, respectively. Each figure presents results showing the effect of differing uniform adhesive thickness, and gives results at both the insert/adhesive and adhesive/plate interfaces. The interaction of the maximum adhesive radial (peel) and shear stresses, with normalised maximum plate stress, showing the effect of adhesive moduli and thickness, is given in Figure 6. To help clarify the trends, additional results for another value of adhesive modulus are also given in this figure.

3.4 Analysis and results for cases with varying adhesive thickness

The adhesive stresses in polar co-ordinates (r,θ), are given in Figures 7 and 8 for the two different adhesives, types A and B, respectively. In each figure results are presented showing the effect of adhesive thickness variation with angular position θ. Results are given at both the insert/adhesive and adhesive/plate interfaces. The interaction of the maximum adhesive radial and shear stresses, with the normalised maximum plate stresses, showing the effect of variation in adhesive moduli and thickness, is given in Figure 9.

4. Plate with bonded oval insert

4.1 Finite element modelling details

A schematic for this reinforcement case is shown in Figure 10. For all cases the radii at the ends of the oval hole boundary are kept as $r_h = 4\,\text{mm}$ with the extension length l allowed to vary such that 3.9 mm $< l < 11.9$ mm. For all cases the insert inner radius is constant at $r_{ii} = 2.9\,\text{mm}$. However, to accommodate cases of varying adhesive thickness around the plate hole boundary, the location of the insert/adhesive interface is defined as follows:

for

$$0 < Y < l; \qquad X = 4 - t_a^{(\theta=0)} \tag{2}$$

$$l < Y; \quad \left(\frac{x}{4 - t_a^{(\theta=0)}}\right)^2 + \left(\frac{y}{4 - t_a^{(\theta=90)}}\right)^2 = 1 \quad \text{where} \quad x = X, \quad \text{and} \quad y = Y - l \tag{3}$$

The finite element meshes consisted of between 600 and 1056 elements. These included 8-noded rectangular iso-parametric elements as well as 6-noded triangular iso-parametric elements. A typical mesh is shown in Figure 11. The adhesive was modelled using one layer of elements. Type A adhesive only was used in all cases. Figure 6, for the circular insert cases (which also used type B adhesive), shows an essentially linear relationship between E_a, t_a and other key variables. Hence it was believed sufficient to consider only one type of adhesive, i.e. one value of E_a, in other work. This aspect is further discussed in Section 6.1.

4.2 Benchmark cases for bounding and validation

For the open hole (unbonded) case with $l = 3.9\,\mathrm{mm}$, the stress concentration factor was determined by the finite element analysis as $K^u = 2.46$, while for $l = 11.9\,\mathrm{mm}$, $K^u = 2.32$. A lower bound for the repaired plate stress concentration factor, K^b, can be obtained by assuming the insert is rigidly connected to the plate, in this case the finite element analysis gives $K^b = 1.16$ for $l = 3.9\,\mathrm{mm}$, and $K^b = 1.39$ for $l = 11.9\,\mathrm{mm}$. No analytical solutions were found in the literature for these cases.

4.3 Analysis and results for cases with constant adhesive thickness

The adhesive stresses in polar co-ordinates (r,α), are given in Figures 12 and 13 for adhesive type A, for two different extension lengths respectively. Each figure presents results showing the effect of adhesive thickness. Results are given at both the insert/adhesive and adhesive/plate interfaces. The interaction of maximum adhesive radial and shear stresses, with normalised maximum plate stress, showing the effect of adhesive thickness and extension length, is given in Figure 15.

4.4 Analysis and results for cases with varying adhesive thickness

The adhesive stresses in polar co-ordinates (r,α), are given in Figure 14 for adhesive type A, for extension length $l = 11.9\,\mathrm{mm}$. Each figure presents results showing the effect of adhesive thickness variation. It should be noted that the adhesive thickness variation occurs around the radiused end of the oval hole. Results are given at both the insert/adhesive and adhesive/plate interfaces. The interaction of the maximum adhesive radial and shear stresses, with normalised maximum plate stress and adhesive thickness variation, is given in Figure 15.

5. Plate with bonded elliptical insert

5.1 Finite element modelling details

A schematic for this reinforcement case is shown in Figure 16. For all cases the plate hole boundary is defined as

$$\left(\frac{X}{4}\right)^2 + \left(\frac{Y}{12}\right)^2 = 1 \tag{4}$$

For all cases the insert inner radius is constant at $r_{ii} = 2.9\,\text{mm}$. However, to accommodate cases of varying adhesive thickness around the plate hole boundary, the location of the insert/adhesive interface is defined as follows:

$$\left(\frac{X}{4 - t_a^{(\alpha=0)}}\right)^2 + \left(\frac{Y}{12 - t_a^{(\alpha=90)}}\right)^2 = 1 \tag{5}$$

It should be noted that in comparison to the previous cases considered, the average adhesive thickness is significantly greater. The finite element mesh consisted of approximately 1300 elements, comprising 8-noded rectangular iso-parametric elements, and 6-noded triangular iso-parametric elements. A typical mesh is shown in Figure 17. Due to the large thickness of adhesive, between 3 and 6 layers of elements were used to model it. As for the oval hole, properties for the adhesive type A were used for all analyses.

5.2 Benchmark cases for bounding and validation

For the open hole (unbonded) case, the stress concentration factor was obtained from the finite element analysis as $K^u = 1.8$, for the finite width plate. This compares well with $K^u = 1.67$ obtained from ESDU [10] for an infinite plate.

5.3 Analysis and results for cases with varying adhesive thickness

The adhesive stresses in local coordinates, normal to the interface shape, which is defined in polar co-ordinates (r, α), are given in Figure 18 for adhesive type A. The results showing the effect of adhesive thickness variation are given at both the insert/adhesive and adhesive/plate interfaces. The interaction of the maximum adhesive radial and shear stresses with normalised maximum plate stresses, showing the effect of adhesive thickness variation, is shown in Figure 19.

6. Discussion of results

6.1 Plate with bonded circular insert

(i) Constant adhesive thickness cases

All radial and tangential adhesive stresses are tensile. It can be seen that the peak shear stresses occur near $\theta = 45^o$. There is a small difference between adhesive stresses at the insert/adhesive and adhesive/plate interfaces, the difference increasing with increase in adhesive thickness, as expected. As the adhesive thickness is increased all stress components reduce. Conversely, as the adhesive modulus is increased all adhesive stresses are increased. As expected, to achieve a reduction in the normalised maximum plate stress, the maximum radial and shear adhesive stresses are increased. Interestingly, irrespective of E_a and t_a, there is very close to a linear relationship between normalised maximum plate stress and maximum adhesive radial stress. It is reasonable to assume that this would apply for other plate and insert material property and similar geometry cases. Similarly there is also a close to linear relationship between normalised maximum plate stress and maximum adhesive shear stress.

(ii) Variable adhesive thickness cases

Again all adhesive radial and tangential stresses are tensile. It can be seen that unlike the constant thickness cases, the location of peak shear stresses moves away from $\theta = 45^o$, and that for a given geometry there is more difference between stresses at the insert/adhesive and adhesive/plate interfaces. As before, when the adhesive modulus is increased all adhesive stresses are increased. It is clear from Figure 9, that the adhesive thickness variation 2 is significantly better than that of variation 1 for reducing both plate and adhesive stresses, irrespective of the adhesive modulus.

6.2 Plate with bonded oval insert

(i) Constant adhesive thickness cases

Unlike the circular insert case, the radial stresses become negative for a reasonable region, and there is no stress peak at the $\theta = 45^o$ location. Also it can be seen that unlike the circular insert case, there is a pronounced peak in radial stress at $\theta = 90^o$. There is also a prominent change in the radial stress distribution in the curved region, for the case of $l = 11.9$ mm. It is believed this is due to the change in local geometry. Again there is little difference between adhesive stresses at the insert/adhesive and adhesive/plate interfaces. As the adhesive thickness is increased all stress components reduce. It is clear that the increased extension length is detrimental for both plate and adhesive stresses, irrespective of the adhesive thickness.

(ii) Variable adhesive thickness cases

The radial stress results have a similar trend to those of constant adhesive thickness cases, however, there is a greater difference between the radial stresses at the insert/adhesive and adhesive/plate interfaces where the adhesive thickness increases. Similarly, hoop and shear adhesive stresses have a significant variation across the adhesive thickness in this region. The shear stresses remain relatively high for a minimal reduction in plate stresses.

6.3 Plate with bonded elliptical insert

The radial and hoop stresses become negative for a reasonable region, and there is a positive shear stress peak in the region of $\theta = 70^o$ to $\theta = 80^o$. Also it can be seen that unlike the circular insert case, there is a pronounced peak in radial stresses at $\theta = 90^o$. There is little difference between adhesive stresses at the insert/adhesive and adhesive/plate interfaces for the locations of 0° to 70° around the hole. From a stress analysis perspective the use of an elliptical insert is the best option. A significant contributing factor is of course the fact that the stress concentration factor for the open elliptical hole is 1.8, as compared to 3.14 for the open circular hole.

7. Conclusions

In this report the emphasis has been directed towards minimising the magnitude of adhesive and maximum plate stresses, and studying the effect of key parameters including (i) insert shape, and (ii) adhesive modulus and thickness. Analyses and results have been presented for circular, oval, and elliptical insert cases. It has been shown that changing the key variables can improve the efficiency of such repairs. Some of the main conclusions that can be drawn from this work include the following:

(i) In general, for a particular shape of reinforcement there is a trade-off between plate and adhesive stresses. This is such that minimising adhesive stresses generally reduces the beneficial effect on plate stresses of the bonded reinforcement.

(ii) For all repairs considered, there was very little difference between adhesive stresses at the insert/adhesive and adhesive/plate interfaces, unless the adhesive layer was quite thick.

(iii) For the circular insert case, for a given value of adhesive modulus, a value of adhesive thickness can be chosen such that there is a relationship very close to linear between normalised maximum plate stress and maximum adhesive radial stress. Similarly there is close to a linear relationship between normalised maximum plate stress and maximum adhesive shear stress. For a given selection of relative plate and insert

(iv) For the circular insert case there was negligible advantage in having a non uniform distribution of adhesive thickness around the boundary.

(v) The results for the oval hole case indicated no real benefit compared to the circular insert case, due to very high local radial stresses.

(vi) To achieve a significant reduction in plate stress concentration, while attaining relatively low adhesive stresses, the elliptical insert is the best option from a stress analysis viewpoint. A significant contributing factor to this is the fact that the stress concentration factor for the open elliptical hole is 1.8, as compared to 3.14 for the open circular hole. It is reasonable to expect that the more slender the ellipse, the better the results will be. Due to the greater difficulty in machining an elliptical shape however, the practical and economic value of his approach is restricted.

8. References

1. **JONES, R. and CALLINAN, R. J. (1981)** *New thoughts on stopping cracks which emanate from holes.* International Journal of Fracture, Vol. 17, R53-R55.

2. **MANN, J.Y., PELL, R.A., JONES, R. and HELLER, M. (1984)** *The use of adhesively bonded inserts to reduce the effects of rivet holes on fatigue life.* Aeronautical Research Laboratory, Structures Report, No. 399.

3. **HELLER, M., JONES R. and WILLIAMS, J.F. (1986)** *Analysis of bonded inserts for the repair of fastener holes.* Journal of Engineering Fracture Mechanics, Vol. 24, pp. 523-532.

4. **HELLER, M., JONES R. and WILLIAMS, J.F. (1989)** *Numerical analysis of bonded repairs for fastener holes with three-dimensional cracks.* Journal of Engineering Fracture Mechanics, Vol. 33 pp. 81-90.

5. **HELLER, M., HILL, T.G., WILLIAMS, J.F. and JONES, R. (1989)** *Increasing the fatigue life of cracked fastener holes using bonded repairs.* Journal of Engineering Fracture Mechanics, Vol. 33 pp. 81-90.

6. **POOLE, P. (1991)** *Personal communication.* AMRL File B2/97, letter 23/12/91.

7. **FINNEY, J.M. (1991)** *Personal communication.* AMRL File B2/97, letter 23/8/91.

8. **PETERSON, R.E. (1974)** *Stress concentration factors.* John Wiley & Sons, Inc.

9. **KOPLIC, B. and KLASSEN, D. D. (1971)** *Reduction of alternating stress range around holes by use of inserts.* Journal of Engineering for industry, pp. 683-687.

10. **ESDU (1995)** *Elastic stress concentration factors. Single reinforced and unreinforced holes on infinite plates of isotropic materials,* Data item 80027, ESDU international, London.

Figures

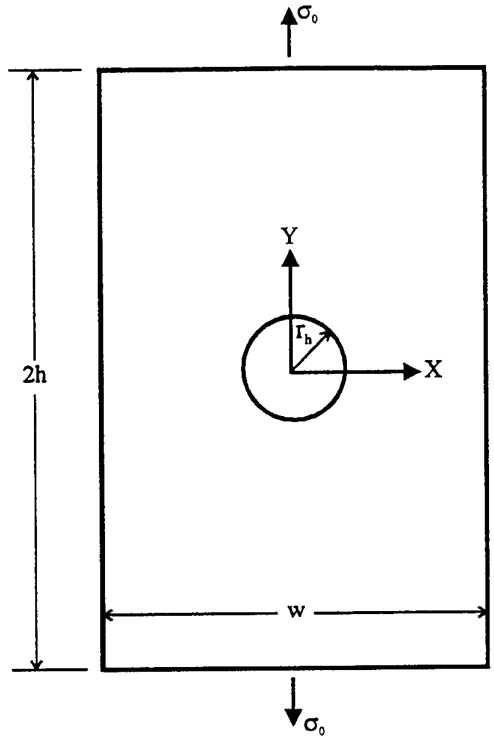

Figure 1. Geometry of specimen with circular hole.

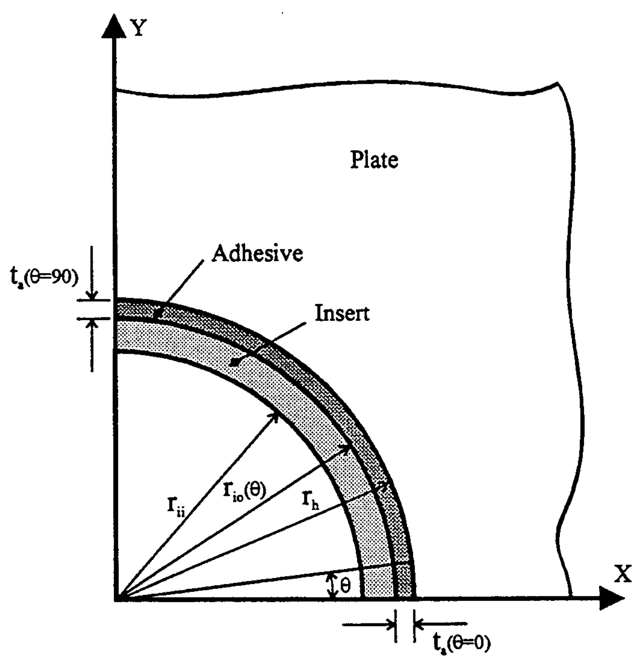

Figure 2. Schematic of region around hole for circular insert case for constant or variable adhesive thickness.

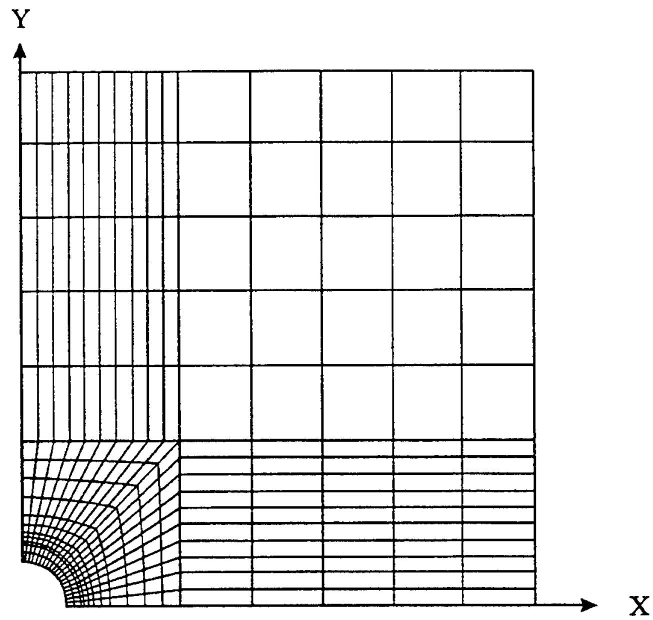

(a) Overall model

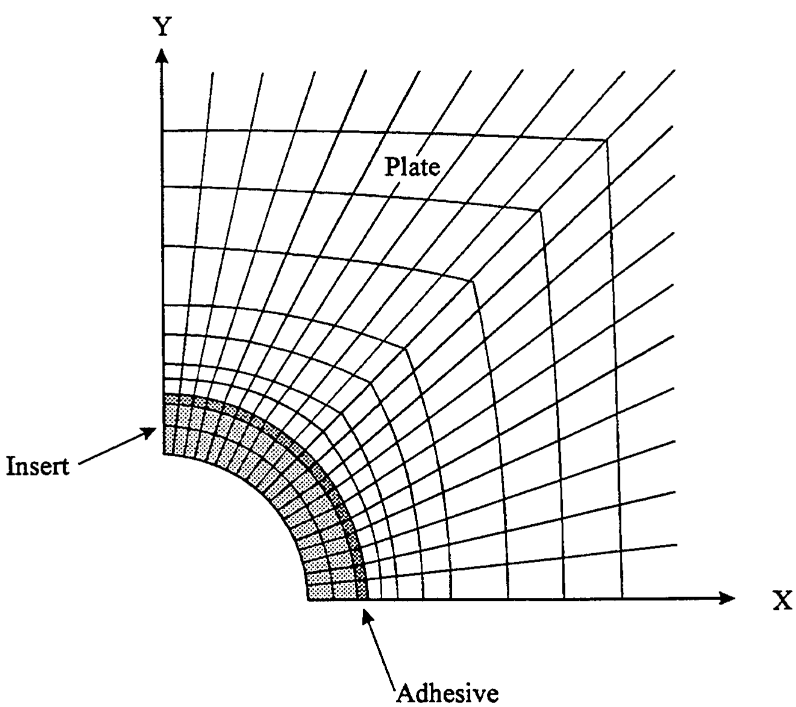

(b) Region around hole

Figure 3. Typical finite element model for plate with circular insert.

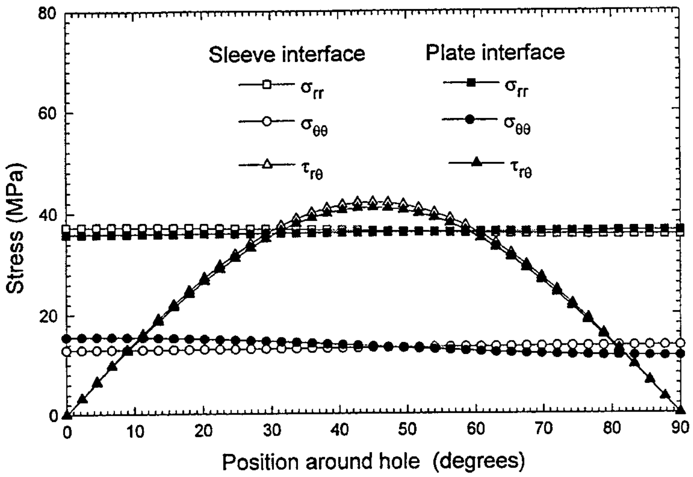

(a) $t_a = 0.05\,\text{mm}$

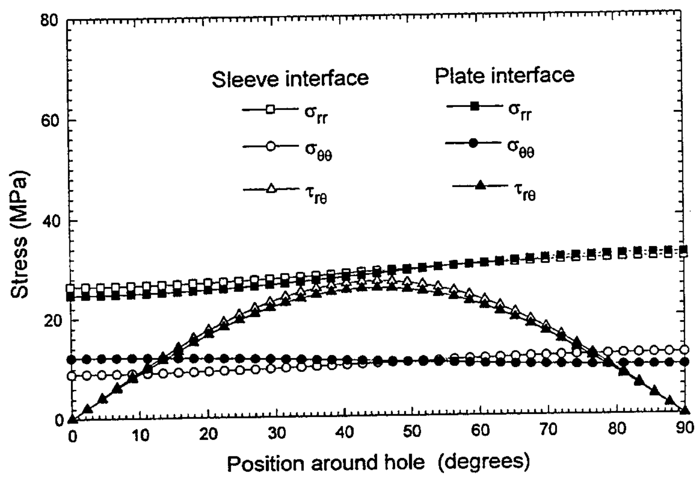

(b) $t_a = 0.1\,\text{mm}$

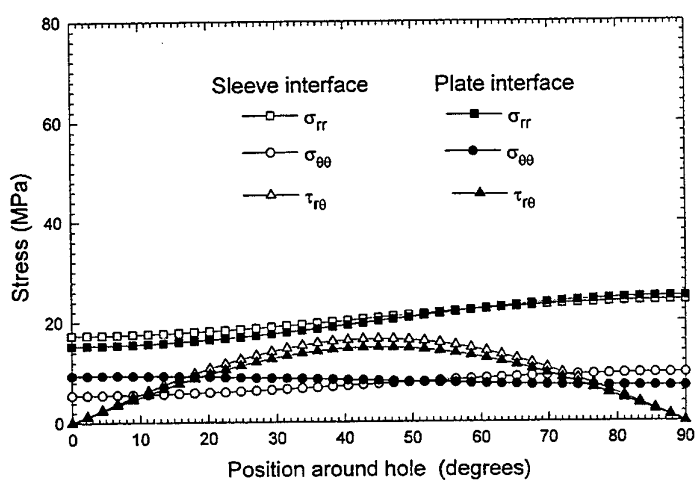

(c) $t_a = 0.2\,\text{mm}$

Figure 4. Adhesive stresses for circular insert with constant adhesive thickness for $E_a = 945$ MPa, $\nu_a = 0.35$ and remote plate stress of $\sigma_o = 115$ MPa.

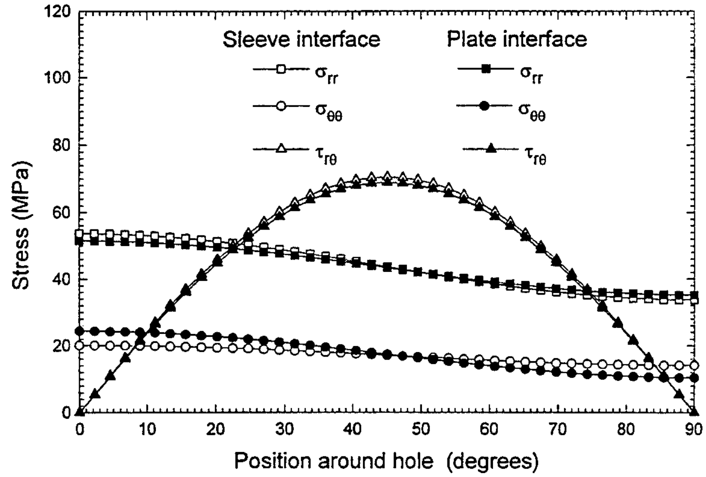

(a) $t_a = 0.05\,\text{mm}$

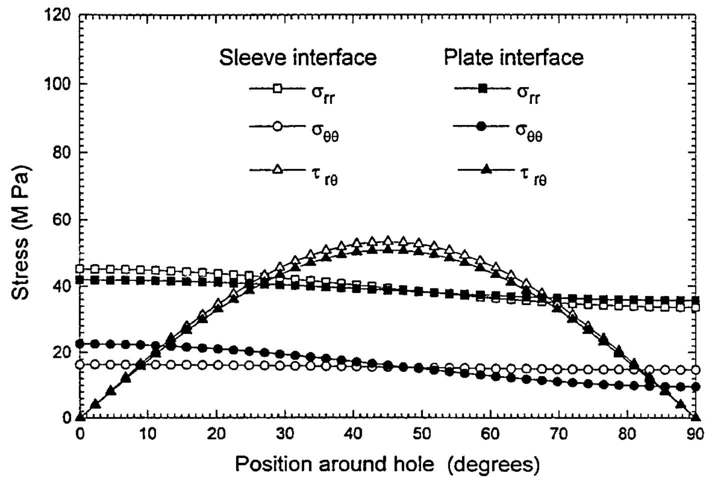

(b) $t_a = 0.1\,\text{mm}$

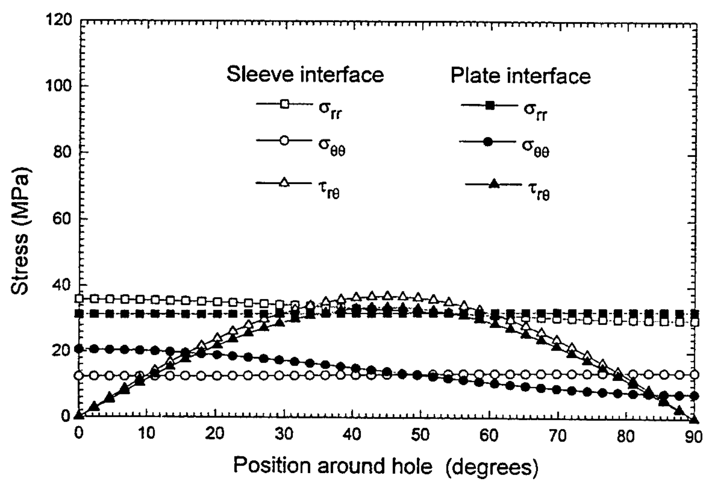

(c) $t_a = 0.2\,\text{mm}$

Figure 5. Adhesive stresses for circular insert with constant adhesive thickness for $E_a = 2758$ MPa, $\nu_a = 0.35$ and remote plate stress of $\sigma_o = 115\,\text{MPa}$.

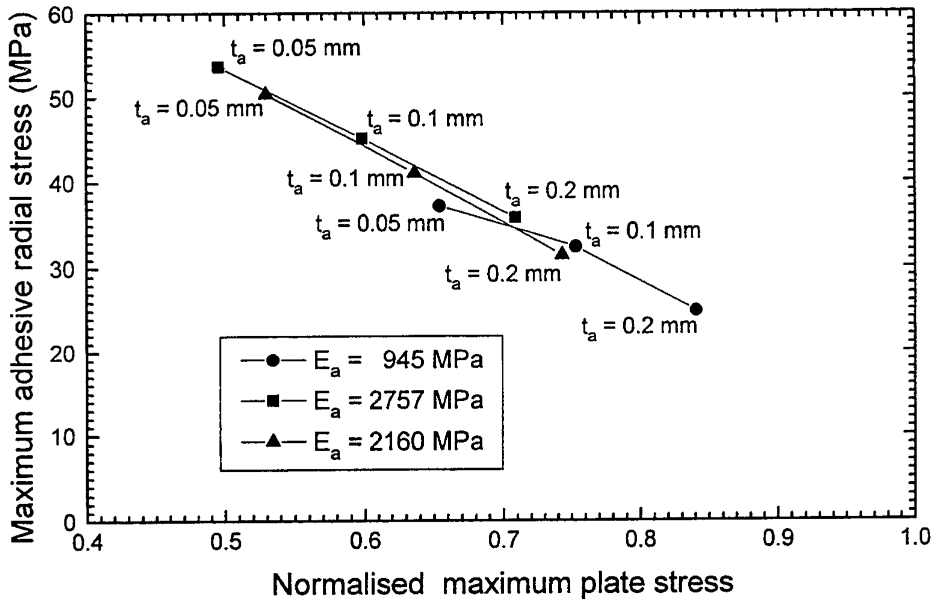

(a) Radial stresses σ_{rr}

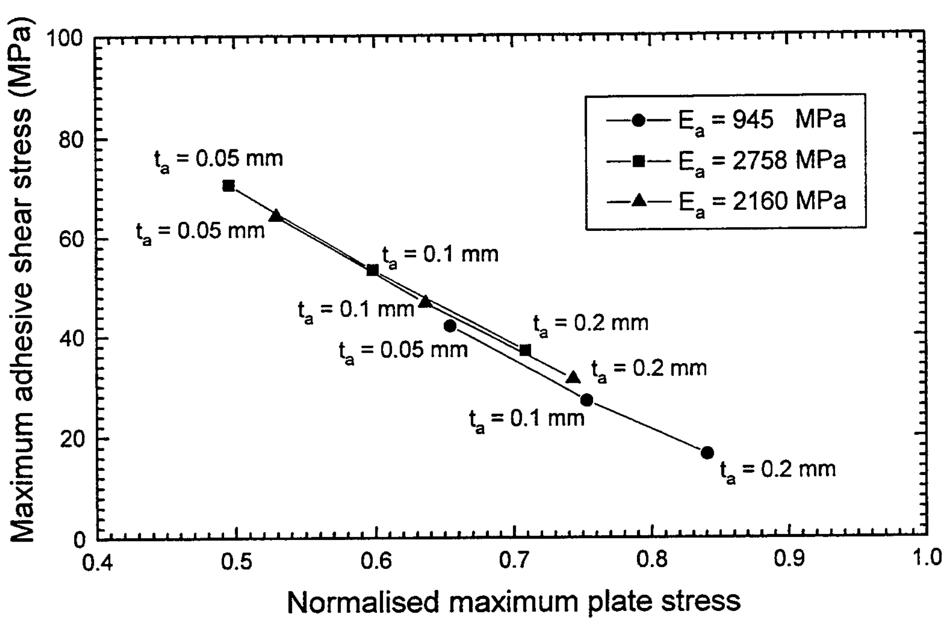

(b) Shear stresses $\tau_{r\theta}$

Figure 6. Maximum adhesive stresses versus normalised maximum plate stresses for circular insert showing effect of adhesive moduli and thickness. Remote plate stress is $\sigma_o = 115\,\text{MPa}$.

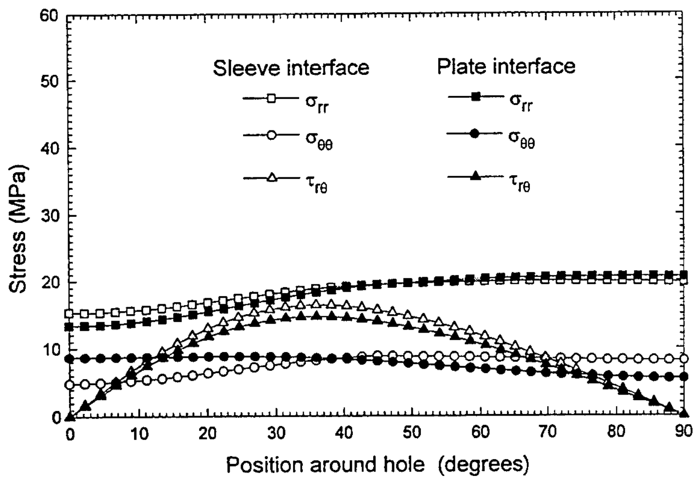

(a) Adhesive thickness variation 1, with $t_a^{\theta=0} = 0.15$ mm and $t_a^{\theta=90} = 0.3$ mm

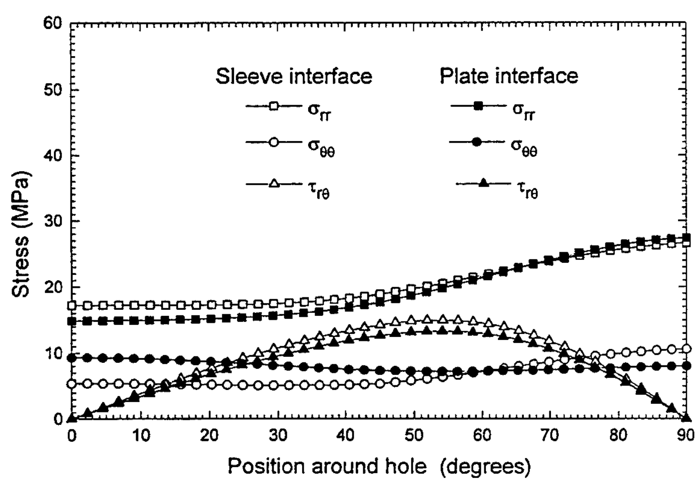

(b) Adhesive thickness variation 2, with $t_a^{\theta=0} = 0.3$ mm and $t_a^{\theta=90} = 0.15$ mm

Figure 7. Adhesive stresses for circular insert with varying adhesive thickness for $E_a = 945$ MPa, $\nu_a = 0.35$ and remote plate stress of $\sigma_o = 115$ MPa.

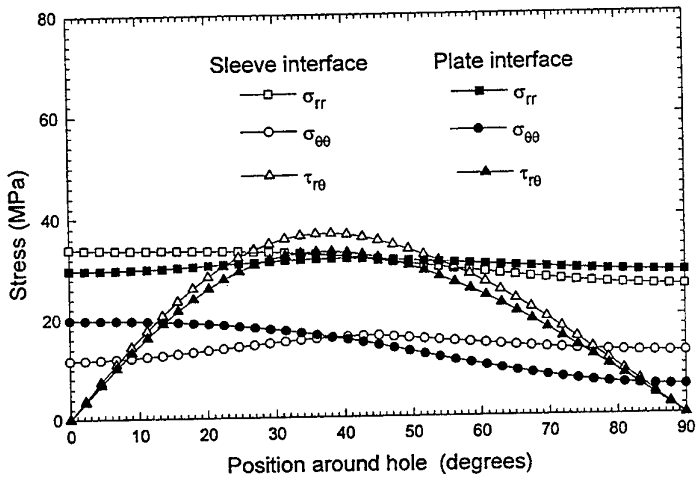

(a) Adhesive thickness variation 1, with $t_a^{\theta=0} = 0.15$ mm and $t_a^{\theta=90} = 0.3$mm

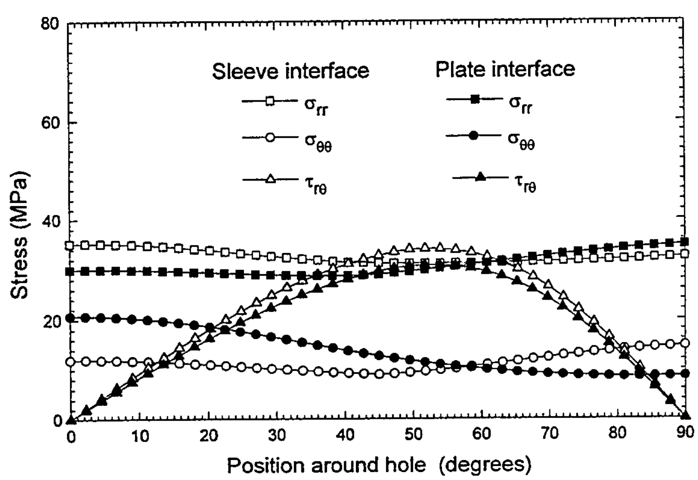

(b) Adhesive thickness variation 2, with $t_a^{\theta=0} = 0.3$ mm and $t_a^{\theta=90} = 0.15$mm

Figure 8. Adhesive stresses for circular insert with varying adhesive thickness for $E_a = 2758$ MPa, $\nu_a = 0.35$ and remote plate stress of $\sigma_o = 115$MPa.

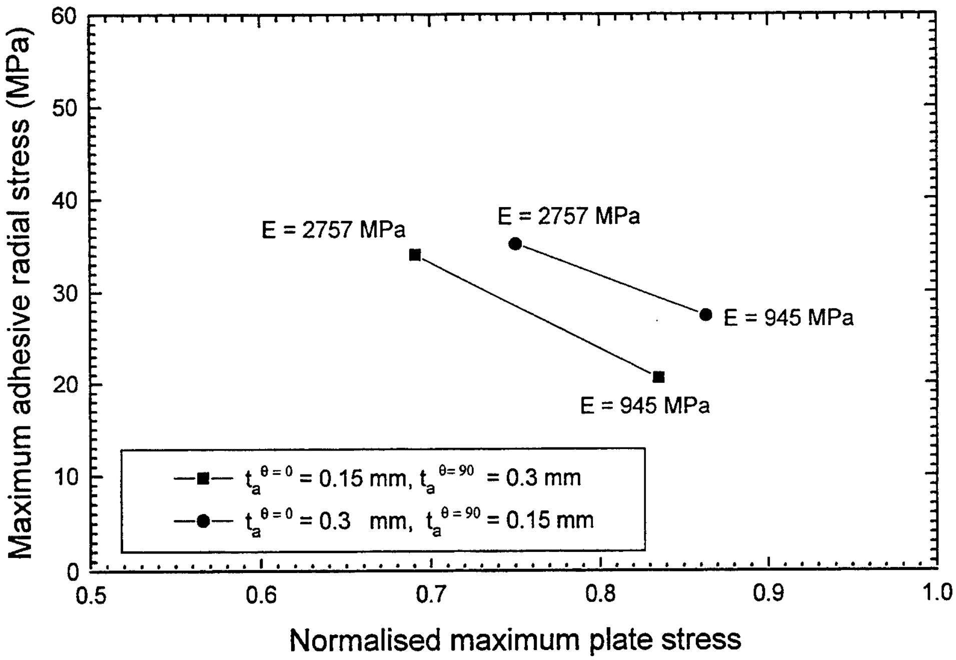

(a) Radial stresses σ_{rr}

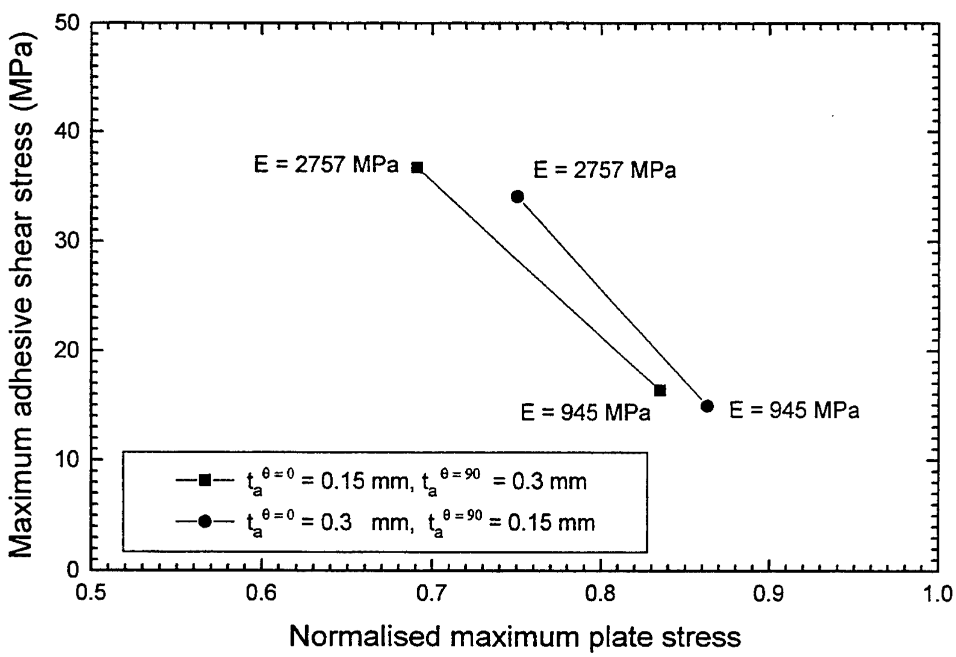

(b) Shear stresses $\tau_{r\theta}$

Figure 9. Maximum adhesive stresses versus normalised maximum plate stresses for circular insert, showing effect of adhesive modulus and thickness. Remote plate stress is $\sigma_o = 115\,\text{MPa}$.

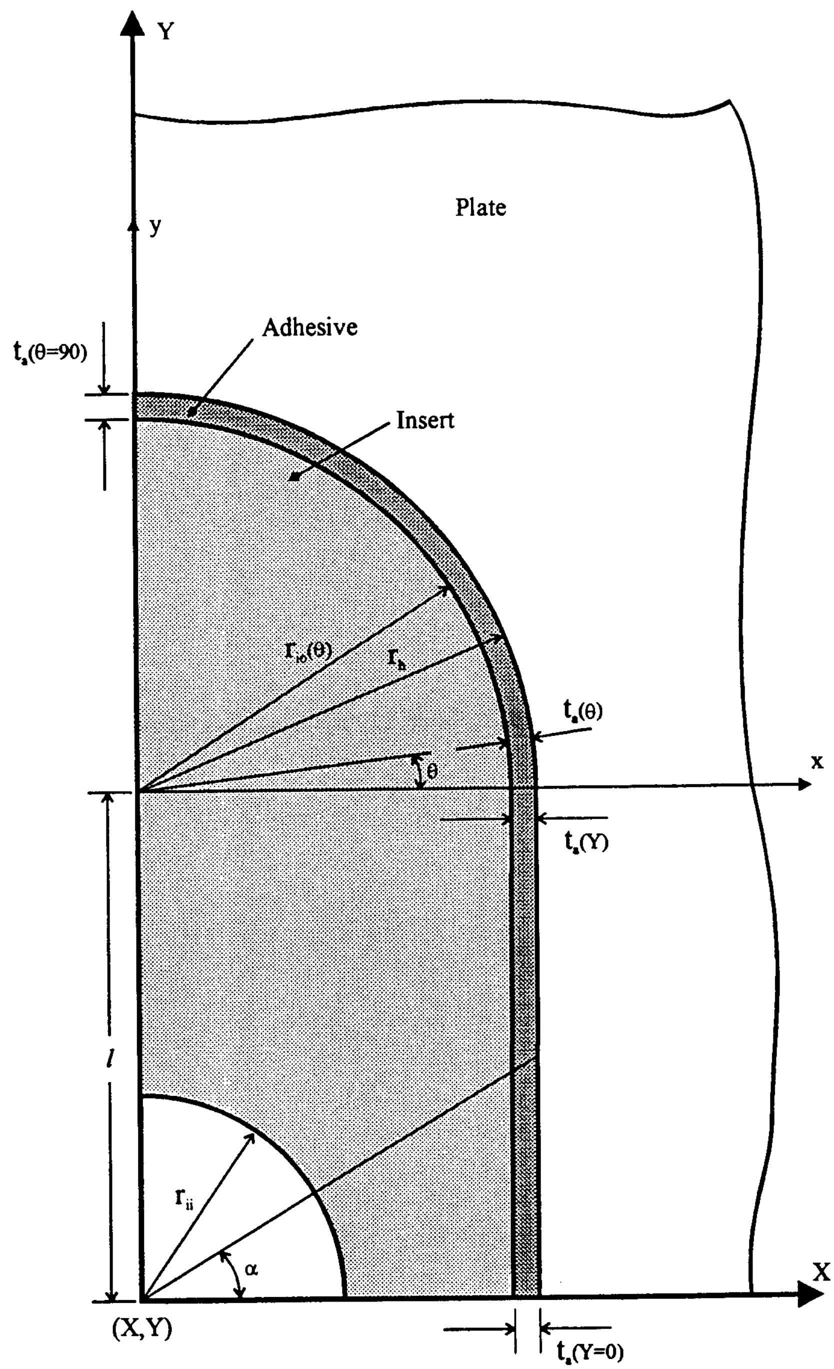

Figure 10. Schematic of region around hole for oval insert case.

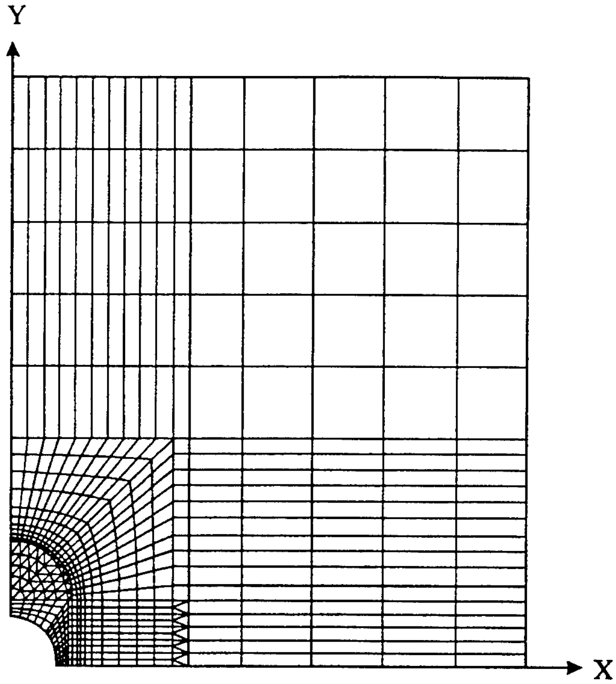

(a) Overall model

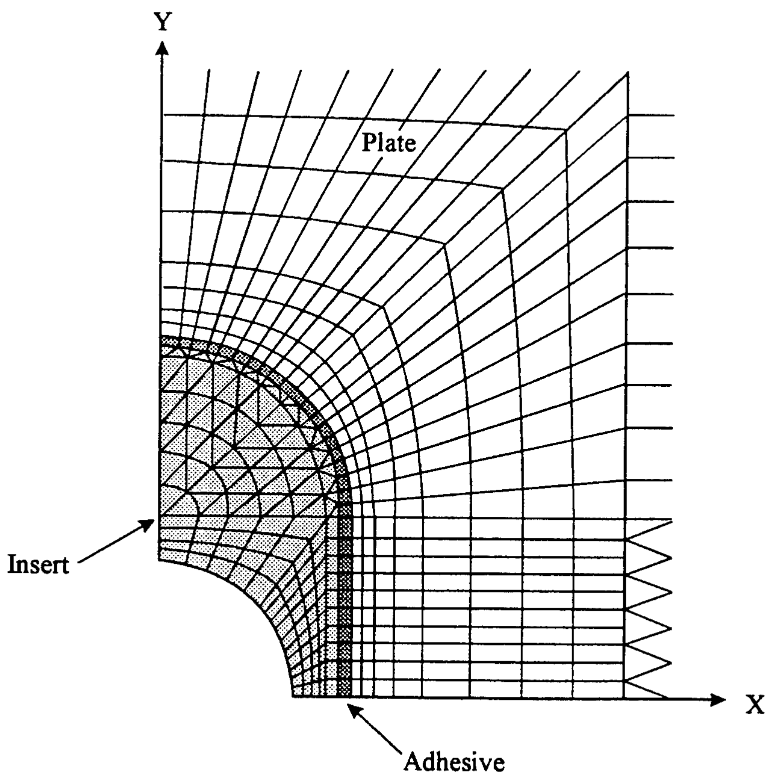

(b) Region around hole

Figure 11. Typical finite element model for plate with oval insert.

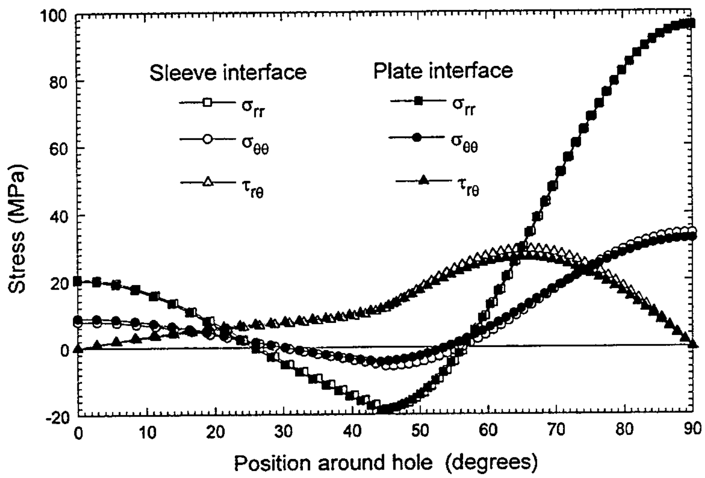

(a) $t_a = 0.1$ mm

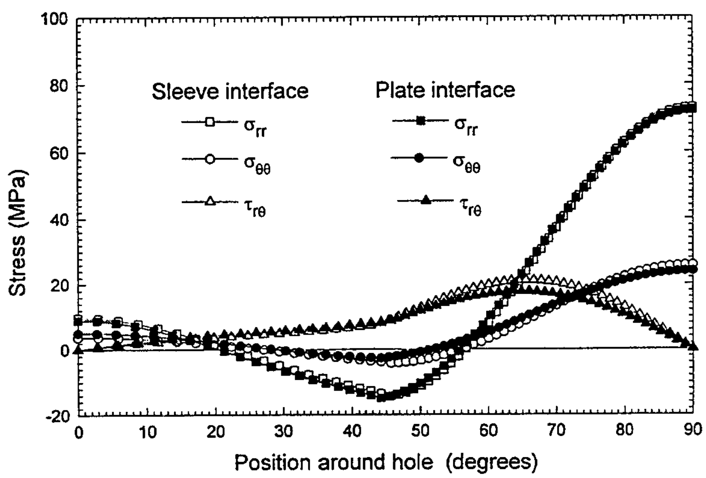

(b) $t_a = 0.2$ mm

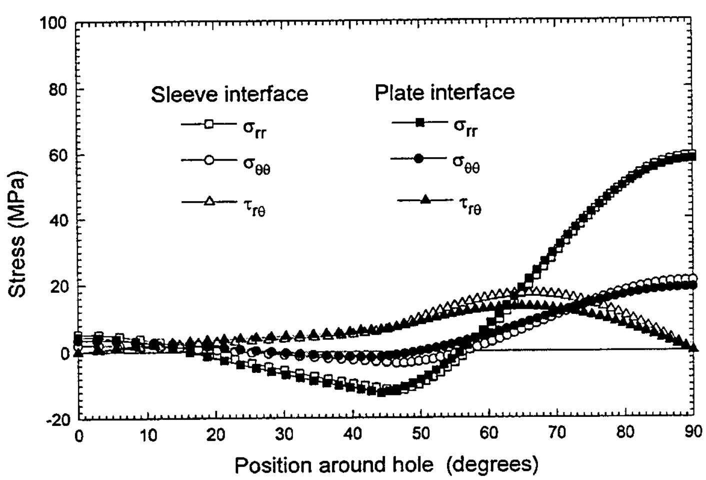

(c) $t_a = 0.3$ mm

Figure 12. Adhesive stresses for oval insert with constant adhesive thickness for $E_a = 945$ MPa, $\nu_a = 0.35$, $l = 3.9$ mm and remote plate stress of $\sigma_o = 115$ MPa.

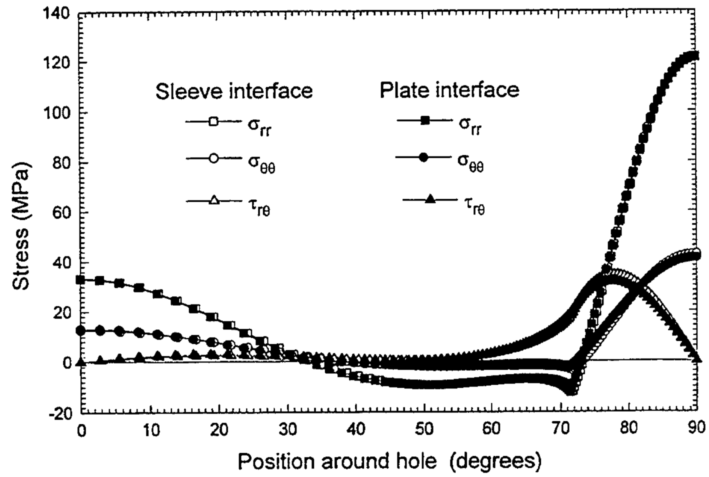

(a) $t_a = 0.1\,\mathrm{mm}$

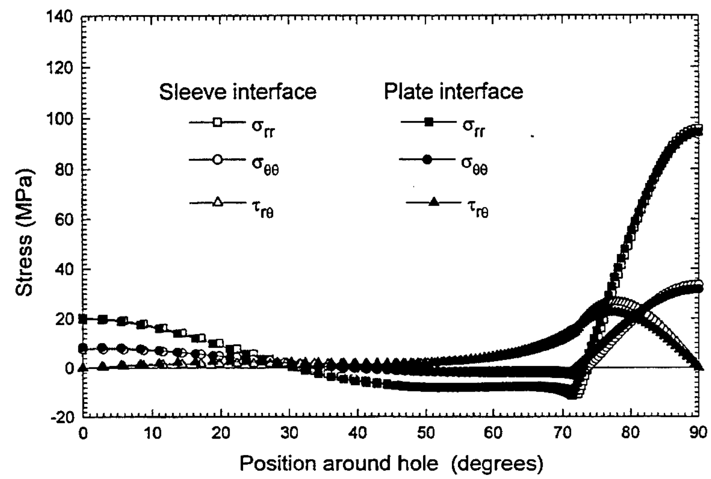

(b) $t_a = 0.2\,\mathrm{mm}$

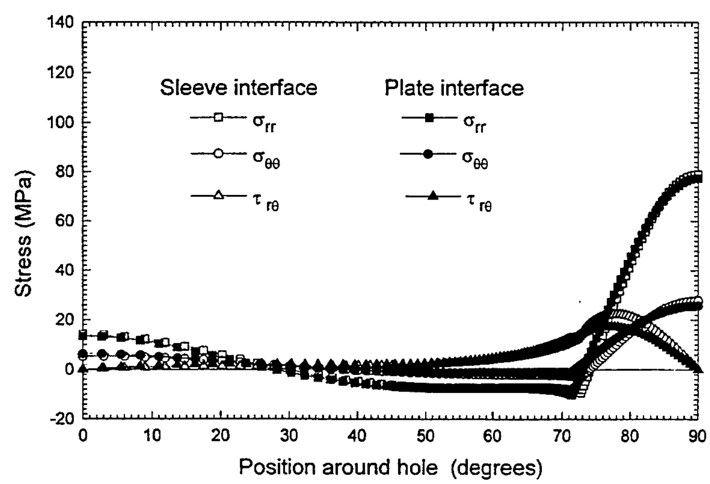

(c) $t_a = 0.3\,\mathrm{mm}$

Figure 13. Adhesive stresses for oval insert with constant adhesive thickness for $E_a = 945$ MPa, $\nu_a = 0.35$, $l = 11.9\,\mathrm{mm}$ and remote plate stress of $\sigma_o = 115\,\mathrm{MPa}$.

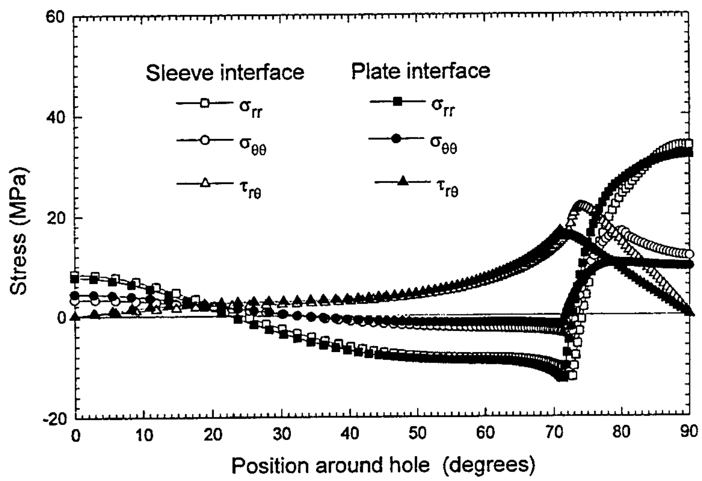

(a) Adhesive thickness variation 3, with $t_a^{\theta=0} = 0.3$ mm and $t_a^{\theta=90} = 1\,\mathrm{mm}$

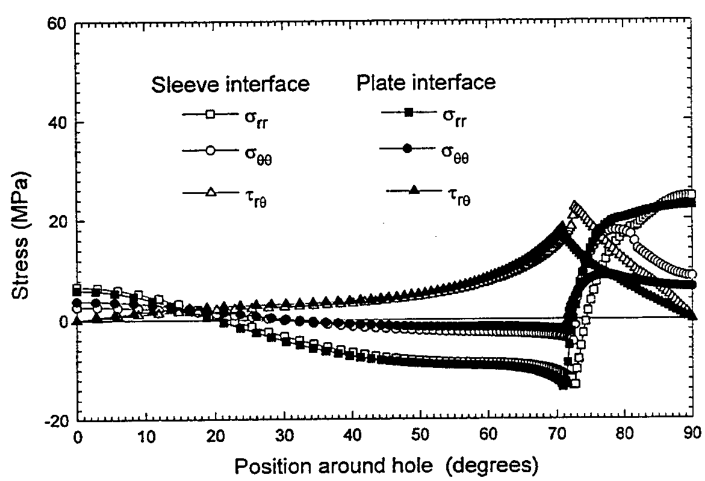

(b) Adhesive thickness variation 4, with $t_a^{\theta=0} = 0.3\,\mathrm{mm}$ and $t_a^{\theta=90} = 1.5$ mm

Figure 14. Adhesive stresses for oval insert with varying adhesive thickness for $E_a = 945$ MPa, $\nu_a = 0.35$, $l = 11.9\,\mathrm{mm}$ and remote plate stress of $\sigma_o = 115\,\mathrm{MPa}$.

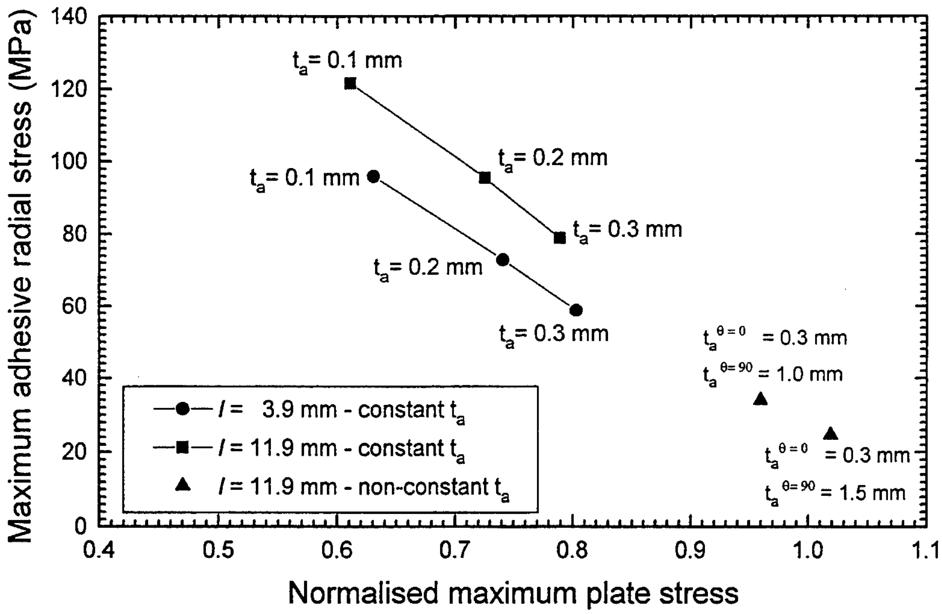

(a) Radial stresses σ_{rr}

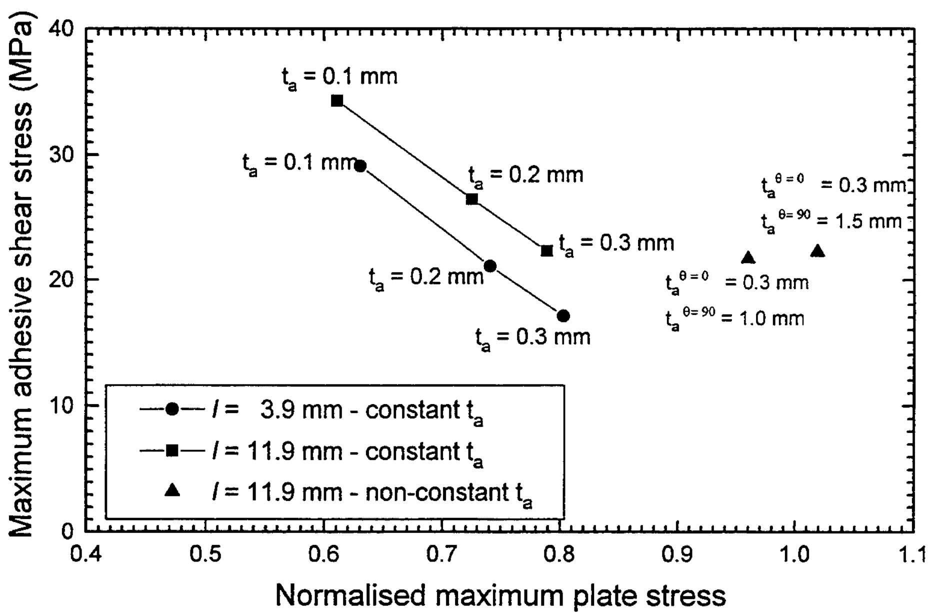

(b) Shear stresses $\tau_{r\theta}$

Figure 15. Maximum adhesive stresses versus normalised maximum plate stresses for oval insert with $E_a = 945$ MPa and $\nu_a = 0.35$, showing effect of variation in adhesive thickness and extension length. Remote plate stress is $\sigma_o = 115$ MPa.

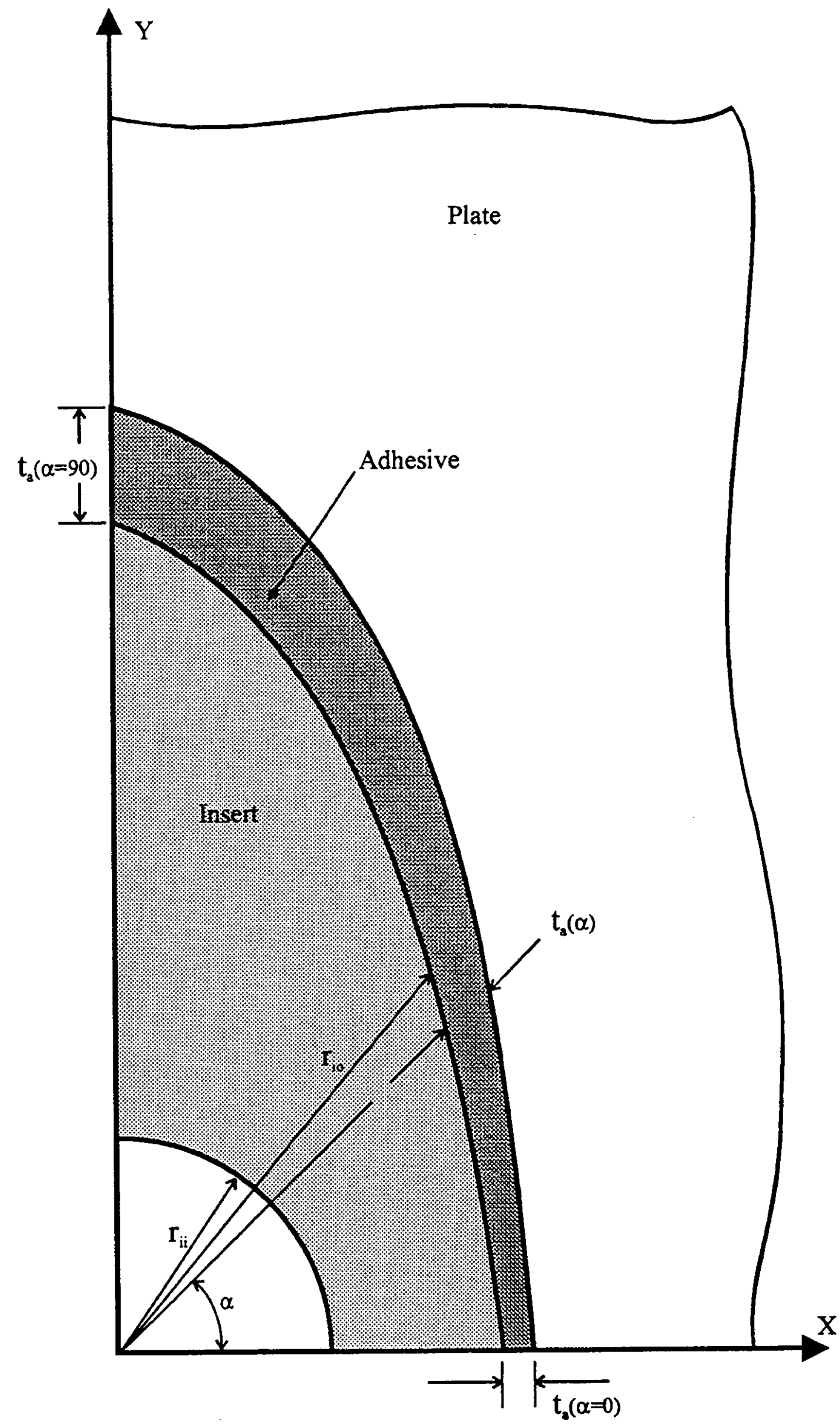

Figure 16. Schematic of region around hole for elliptical insert case.

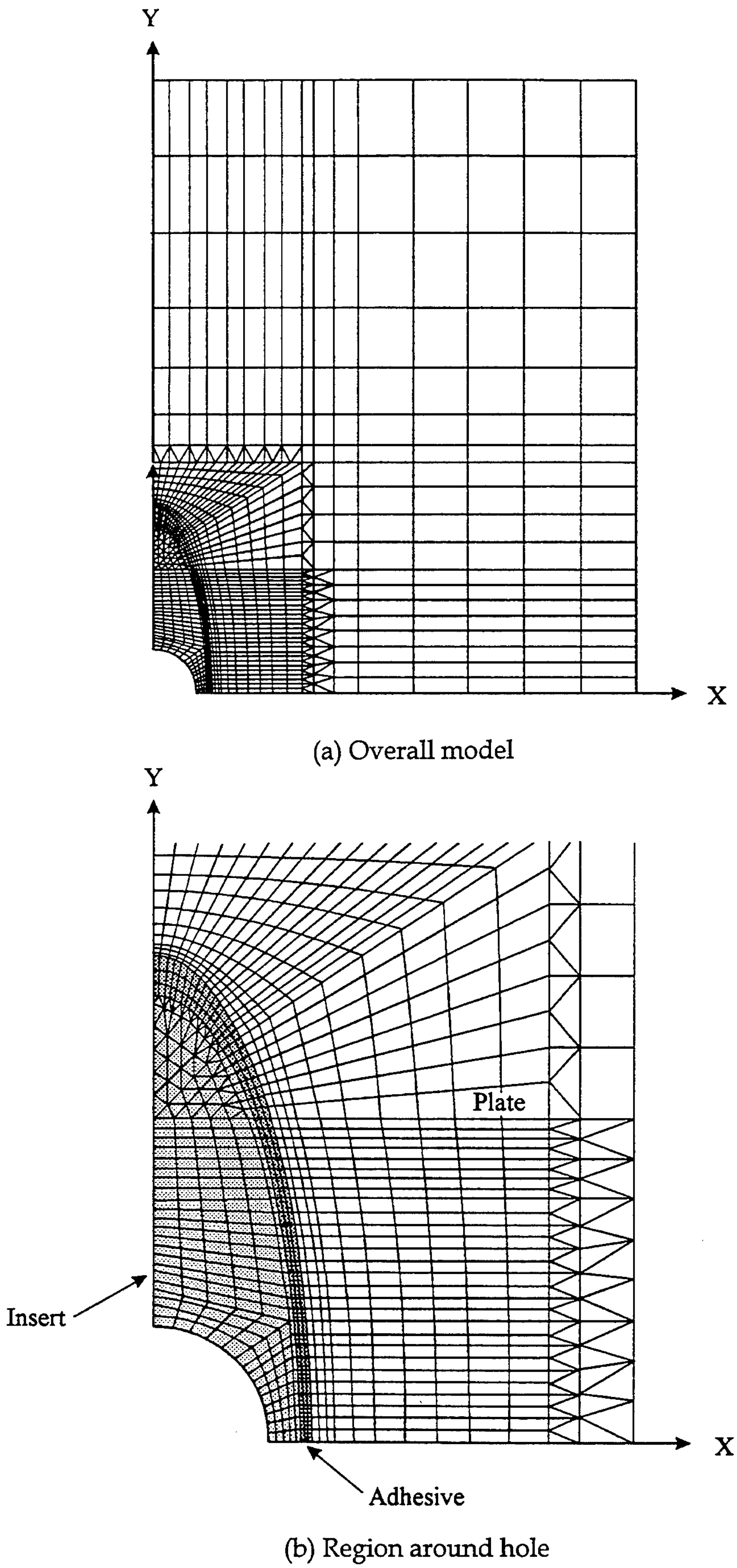

Figure 17. Typical finite element model for plate with elliptical insert.

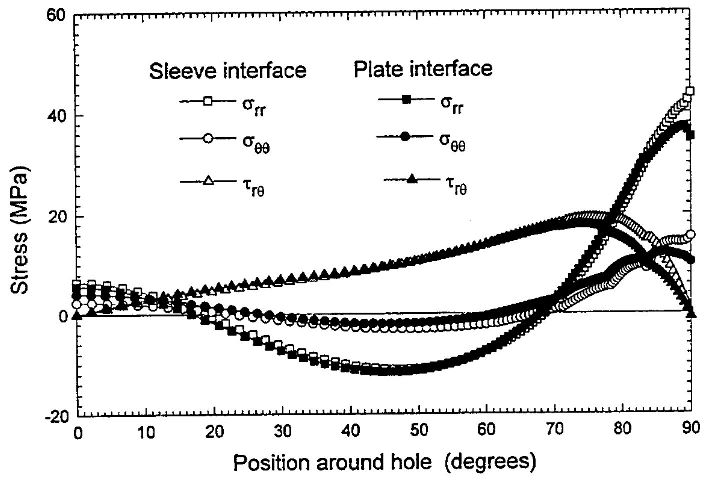

(a) Adhesive thickness variation 5, with $t_a^{\alpha=0} = 0.2$ mm and $t_a^{\alpha=90} = 0.6$ mm

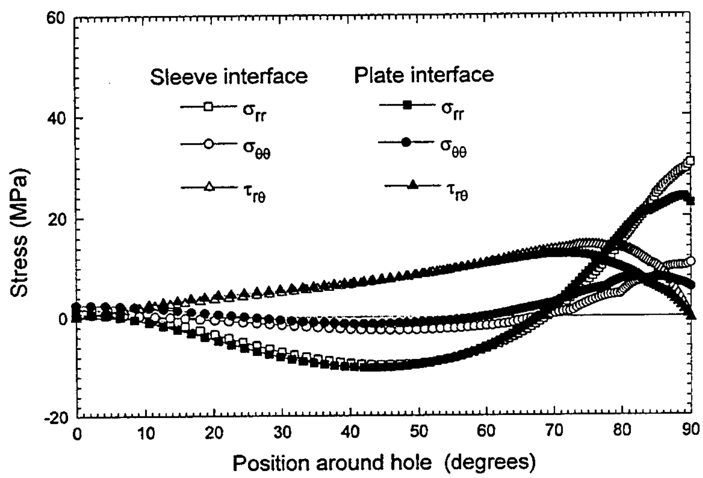

(b) Adhesive thickness variation 6, with $t_a^{\alpha=0} = 0.3$ mm and $t_a^{\alpha=90} = 1$ mm

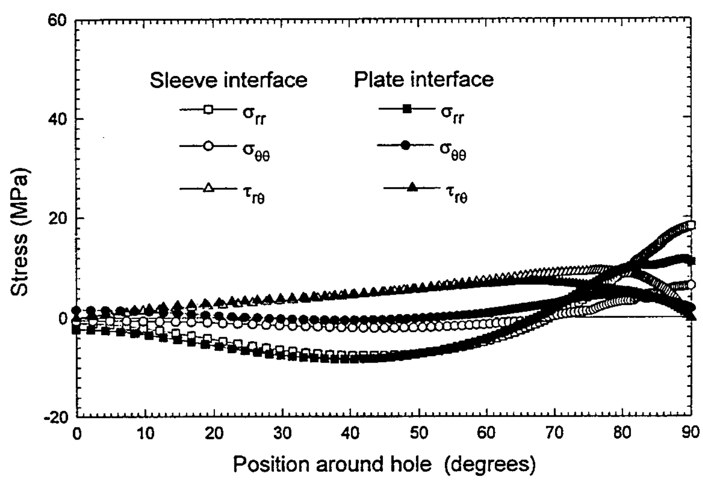

(c) Adhesive thickness variation 7, with $t_a^{\alpha=0} = 0.5$ mm and $t_a^{\alpha=90} = 2$ mm

Figure 18. Adhesive stresses for elliptical insert with varying adhesive thickness for $E_a = 945$ MPa, $\nu_a = 0.35$ and remote plate stress of $\sigma_o = 115$ MPa.

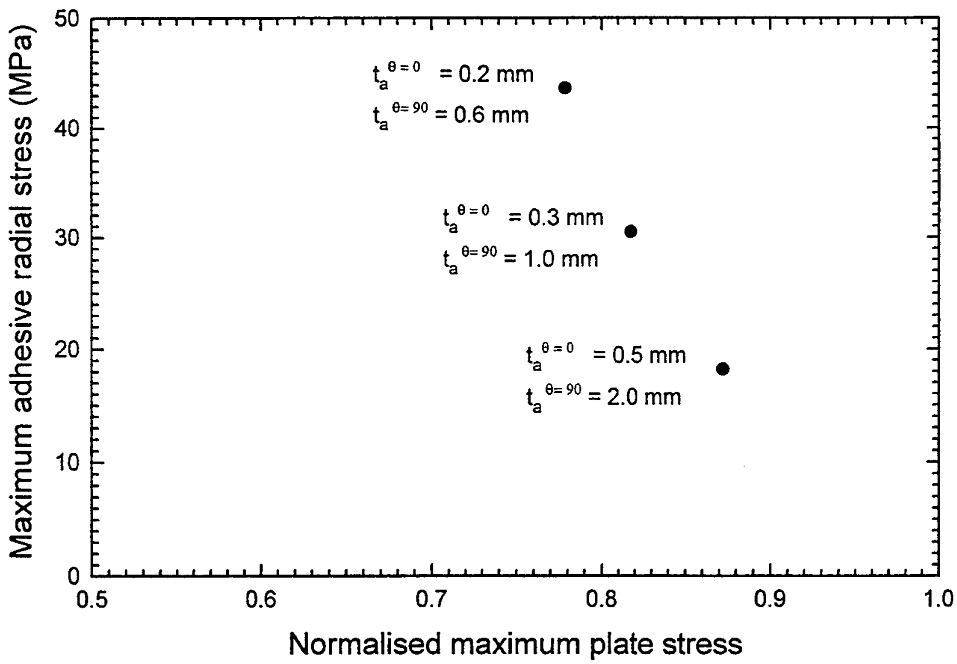

(a) Radial stresses σ_{rr}

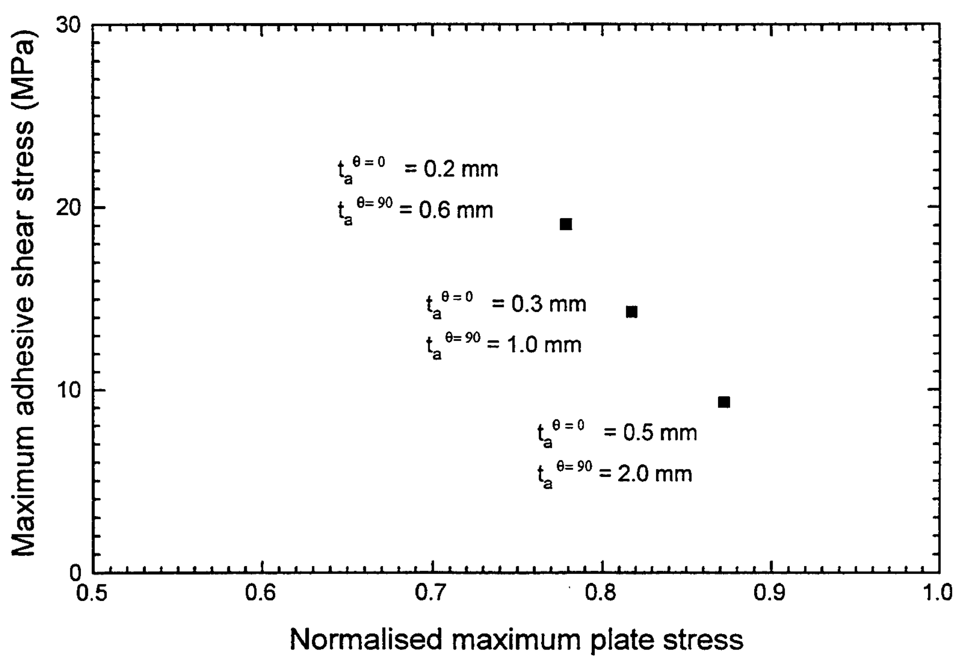

(b) Shear stresses $\tau_{r\theta}$

Figure 19. Maximum adhesive stresses versus maximum normalised plate stresses for elliptical insert showing effect of adhesive thickness variation. Remote plate stress is $\sigma_o = 115$ MPa.

Effect of Bonded Insert Shape and Adhesive Thickness on Critical Stresses in a Loaded Plate

R.L. Evans and M. Heller

DISTRIBUTION LIST

AUSTRALIA

TASK SPONSOR: AIR OIC ASI-LSA

DEFENCE ORGANISATION

Defence Science and Technology Organisation

Chief Defence Scientist
FAS Science Policy
AS Science Industry and External Relations
AS Science and Industry Interaction
} shared copy
Counsellor Defence Science, London (Doc Data Sheet only)
Counsellor Defence Science, Washington (Doc Data Sheet only)
Scientific Adviser to Thailand MRD (Doc Data Sheet Only)
Senior Defence Scientific Adviser/Scientific Adviser Policy and Command (shared copy)
Navy Scientific Adviser (3 copies Doc Data Sheet and 1 copy distribution list)
Scientific Adviser - Army (Doc Data Sheet and distribution list only)
Air Force Scientific Adviser
Director Trials

Aeronautical and Maritime Research Laboratory

Director
Chief of Airframes and Engines Division
Research Leader Fracture Mechanics
T.G. Hill
E. Kowal
C. Pickthall
C. Wang
R.L. Evans
M. Heller

Electronics and Surveillance Research Laboratory

Director

DSTO Library

Library Fishermens Bend
Library Maribyrnong
Library DSTOS (2 copies)
Library, MOD, Pyrmont (Doc Data sheet only)

Forces Executive

Director General Force Development (Sea) (Doc Data Sheet only)
Director General Force Development (Land) (Doc Data Sheet only)
Director General Force Development (Air)

Defence Central

OIC TRS, Defence Central Library
Officer in Charge, Document Exchange Centre (DEC)
US Defence Technical Information Centre, 2 copies
UK Defence Research Information Centre, 2 copies
Canada Defence Scientific Information Service, 1 copy
NZ Defence Information Centre, 1 copy
National Library of Australia, 1 copy
Defence Intelligence Organisation
Library, Defence Signals Directorate (Doc Data Sheet only)

Air Force

OIC ATF ATS, RAAFSTT, WAGGA (2 copies)

Army

ABCA Office, G-1-34, Russell Offices, Canberra (4 copies)

UNIVERSITIES AND COLLEGES

Australian Defence Force Academy
- Library
- Head of Aerospace and Mechanical Engineering

Deakin University, Serials Section (M list)), Deakin University Library, Geelong, 3217

Monash University
- Senior Librarian, Hargrave Library
- Head Materials Engineering

Librarian, Flinders University

Sydney
- Engineering Library
- Head School of Mechanical & Mechatronic Engineering
- Head School of Aeronautical Engineering

Melbourne
- Engineering Library

NSW
- Head, Mechanical Engineering

Tasmania
- Engineering Library

Western Australia
- Head Mechanical Engineering

RMIT
- Library

OTHER ORGANISATIONS

NASA (Canberra)
AGPS
ASTA Engineering, Document Control Office
Hawker de Havilland Aust Pty Ltd, Bankstown, Library
BHP Melbourne Research Laboratories

ABSTRACTING AND INFORMATION ORGANISATIONS

INSPEC: Acquisitions Section Institution of Electrical Engineers
Library, Chemical Abstracts Reference Service
Engineering Societies Library, US
American Society for Metals
Documents Librarian, The Center for Research Libraries, US

INFORMATION EXCHANGE AGREEMENT PARTNERS

Acquisitions Unit, Science Reference and Information Service, UK
Library - Exchange Desk, National Institute of Standards and Technology, US
National Aerospace Laboratory, Japan
National Aerospace Laboratory, Netherlands

UNITED KINGDOM

Defence Research Agency (Aerospace)
Farnborough, Materials and Structures
P. Poole
R. Cook

SPARES 10 copies

TOTAL 76 copies

Page classification: UNCLASSIFIED

DEFENCE SCIENCE AND TECHNOLOGY ORGANISATION
DOCUMENT CONTROL DATA

1. PRIVACY MARKING/CAVEAT (OF DOCUMENT)

2. TITLE

Effect of Bonded Insert Shape and Adhesive Thickness on Critical Stresses in a Loaded Plate

3. SECURITY CLASSIFICATION (FOR UNCLASSIFIED REPORTS THAT ARE LIMITED RELEASE USE (L) NEXT TO DOCUMENT CLASSIFICATION)

Document	(U)
Title	(U)
Abstract	(U)

4. AUTHOR(S)

R.L. Evans and M. Heller

5. CORPORATE AUTHOR

Aeronautical and Maritime Research Laboratory
PO Box 4331
Melbourne Vic 3001

6a. DSTO NUMBER	6b. AR NUMBER	6c. TYPE OF REPORT	7. DOCUMENT DATE
DSTO-TR-0409	AR-009-875	Technical Report	August 1996

8. FILE NUMBER	9. TASK NUMBER	10. TASK SPONSOR	11. NO. OF PAGES	12. NO. OF REFERENCES
M1/9/113	95/228	AIR	28	10

13. DOWNGRADING/DELIMITING INSTRUCTIONS

None

14. RELEASE AUTHORITY

Chief, Airframes and Engines Division

15. SECONDARY RELEASE STATEMENT OF THIS DOCUMENT

Approved for public release

OVERSEAS ENQUIRIES OUTSIDE STATED LIMITATIONS SHOULD BE REFERRED THROUGH DOCUMENT EXCHANGE CENTRE, DIS NETWORK OFFICE, DEPT OF DEFENCE, CAMPBELL PARK OFFICES, CANBERRA ACT 2600

16. DELIBERATE ANNOUNCEMENT

No limitations

17. CASUAL ANNOUNCEMENT Yes

18. DEFTEST DESCRIPTORS

Finite element analysis; Inserts; Plates; Stresses

19. ABSTRACT

This report presents the results of finite element analyses conducted to calculate the magnitude of adhesive stresses for a large plate with a bonded insert, and study the interaction of key parameters including (i) insert shape, and (ii) adhesive modulus and thickness, with maximum plate stresses. Results are presented for circular, oval and elliptical insert cases. It is shown that changing the key variables can improve the efficiency of such repairs, however due to typically high adhesive stresses, careful consideration must be given to the level of applied loading and the design of the insert chosen. In general, for a particular shape of reinforcement, there is a trade-off between plate and adhesive stress magnitudes. This relationship is such that minimising adhesive stresses (through increasing adhesive thickness or reducing adhesive modulus) reduces the beneficial effect on plate stresses of the bonded reinforcement. It is shown that for circular inserts this relationship is essentially linear.

Page classification: UNCLASSIFIED